J|A|C|S
ARTICLES
Published on Web 11/12/2003

An Evaluation of Amide Group Planarity in 7-Azabicyclo[2.2.1]heptane Amides. Low Amide Bond Rotation Barrier in Solution

Yuko Otani,[†] Osamu Nagae,[†] Yuji Naruse,[‡] Satoshi Inagaki,[‡] Masashi Ohno,[§] Kentaro Yamaguchi,[§] Gaku Yamamoto,[||] Masanobu Uchiyama,[†,⊥] and Tomohiko Ohwada*,[†]

Contribution from the Graduate School of Pharmaceutical Sciences, The University of Tokyo, 7-3-1 Hongo, Bunkyo-ku, Tokyo, 113-0033, Japan; Department of Chemistry, Faculty of Engineering, Gifu University, Yanagido, Gifu 501-1193, Japan; Chemical Analysis Center, Chiba University, Yayoi-cho, Inage-ku, Chiba 263-8522, Japan; and Department of Chemistry, School of Science, Kitasato University, Kitasato, Sagamihara, Kanagawa 228-8555, Japan

Received June 12, 2003; E-mail: ohwada@mol.f.u-tokyo.ac.jp

Abstract: Here we show that amides of bicyclic 7-azabicyclo[2.2.1]heptane are intrinsically nitrogen-pyramidal. Single-crystal X-ray diffraction structures of some relevant bicyclic amides, including the prototype *N*-benzoyl-7-azabicyclo[2.2.1]heptane, exhibited nitrogen-pyramidalization in the solid state. We evaluated the rotational barriers about the amide bonds of various *N*-benzoyl-7-azabicyclo[2.2.1]heptanes in solution. The observed reduction of the rotational barriers of the bicyclic amides, as compared with those of the monocyclic pyrrolidine amides, is consistent with a nitrogen-pyramidal structure of 7-azabicyclo[2.2.1]heptane amides in solution. A good correlation was found between the magnitudes of the rotational barrier of *N*-benzoyl-7-azabicyclo[2.2.1]heptanes bearing *para*-substituents on the benzoyl group and the Hammett's σ_p^+ constants, and this is consistent with the similarity of the solution structures. Calculations with the density functional theory reproduced the nitrogen-pyramidal structures of these bicyclic amides as energy minima. The calculated magnitudes of electron delocalization from the nitrogen nonbonding n_N orbital to the carbonyl π^* orbital of the amide group evaluated by application of the bond model theory correlated well with the rotational barriers of a variety of amides, including amides of 7-azabicyclo[2.2.1]heptane. The nonplanarity of the amide nitrogen of 7-azabicyclo[2.2.1]heptanes would be derived from nitrogen-pyramidalization due to the CNC angle strain and twisting of the amide bond due to the allylic strain.

Introduction

An amide bond is a fundamental linkage in proteins and many other kinds of bioactive molecules. Planarity of the amide bond is a general feature of natural and synthetic molecules containing an amide moiety,[1] and this feature frequently determines the overall structures of the molecules. Geometrical transformation with respect to the amide bond can occur through (1) N−C(O) *bond rotation* and (2) *nitrogen inversion* (Scheme 1). The nonplanar structures involved are transitional and are called twisted and pyramidal structures, respectively. These structural changes can occur simultaneously. On the other hand, several examples of nonplanar amides *in the ground state* have been reported (Figure 1).[2−9] They are known as pyramidal amides or twisted amides. There have been studies on the chemical properties and synthesis, as well as ab initio calculations, of bicyclic bridgehead amides (**A**)[2,3] and a tricyclic amide, 1-aza-2-adamantanone (**B**).[4,5] Thioimide derivatives (**C**) have been reported to have a twisted amide structure in the solid state.[6] Aziridine amides (**D**) are the most strained amides.[7] Bisheteroatom-substituted amides (called as anomeric amides) (**E**) are different from normal amides.[8] Their high reactivities of bond

Scheme 1. General Description of Amide Transformation Processes[a]

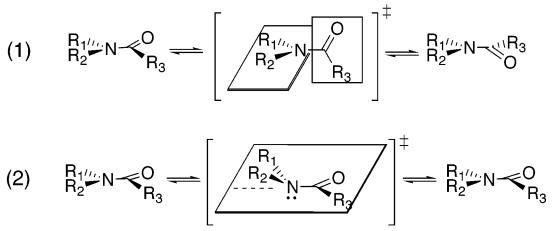

[a] (1) N−C bond rotation and (2) nitrogen pyramidalization.

[†] The University of Tokyo.
[‡] Gifu University.
[§] Chiba University.
[||] Kitasato University.
[⊥] PRESTO, Japan Science and Technology Corporation (JST).

(1) Greenberg, A.; Breneman, C. M. *Amide Linkage*; Liebman, J. F. Ed.; Wiley-Interscience (A Division of John Wiley & Sons): New York, 2000.
(2) (a) Somayaji, V.; Brown, R. S. *J. Org. Chem.* **1986**, *51*, 2676−2686. (b) Wang, Q. P.; Bennet, A. J.; Brown, R. S.; Santariero, B. D. *J. Am. Chem. Soc.* **1991**, *113*, 5757−5765.
(3) (a) Greenberg, A.; Moore, D. T.; Dubois, T. D. *J. Am. Chem. Soc.* **1996**, *118*, 8658−8668. (b) Greenberg, A.; Venanzi, C. A. *J. Am. Chem. Soc.* **1993**, *115*, 6951−6957.
(4) (a) Kirby, A., J.; Komarov, I., V.; Wothers, P., D.; Feeder, N. *Angew. Chem., Int. Ed.* **1998**, *37*, 785−786. (b) Kirby, A. J.; Komarov, I. V.; Feeder, N. *J. Am. Chem. Soc.* **1998**, *120*, 7101−7102. (c) Kirby, A. J.; Komarov, I. V.; Feeder, N. *J. Chem. Soc., Perkin Trans. 2* **2001**, 522−529.

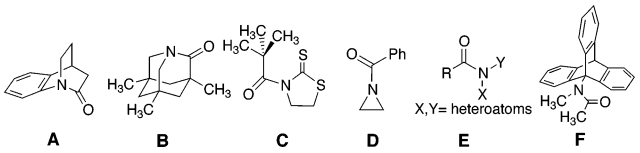

Figure 1. Some examples of nonplanar amides.

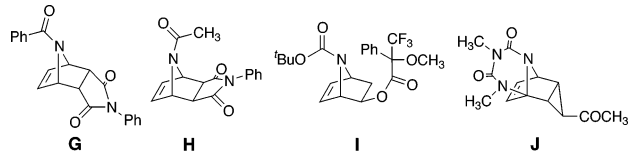

Figure 2. Previously reported 7-azabicyclo[2.2.1]heptane amides.

cleavage of N−X (or N−Y) and nitrogen pyramidalization are observed, which were proposed to be attributed to a negative hyperconjugation (i.e., anomeric) effect within the XNY system. Triptycene derivatives such as *N*-methyl-*N*-9-triptycylacetamide (**F**) were reported to be nitrogen-pyramidal.[9] In the field of medicinal chemistry, cyclophiline and FK506-binding protein (FKBP) are known as enzymes that catalyze the *cis*−*trans* isomerization of prolyl peptide bonds, a process which is postulated to proceed through a stabilized twisted amide structure.[10] Furthermore, the common occurrence of a slight pyramidalization of amide bonds in ubiquitous peptides has been discussed for a long time.[11]

We have been seeking a simple molecular architecture that induces nitrogen-pyramidalization of amides and have shown that the nitrogen atoms of some simple amides of 7-azabicyclo-[2.2.1]heptane (e.g., **1a** and **1e**; see Figure 3) are pyramidalized in the solid state.[12]

Although the crystal structures of amide derivatives of 7-azabicyclo[2.2.1]heptane, **G**,[13] **H**,[13] **I**,[14] and **J**[15] are available in the Cambridge Structural Database (Figure 2), pyramidalized nitrogen in derivatives of 7-azabicyclo[2.2.1]heptane is not well documented or widely recognized, probably because the above examples are sterically biased (sterically unsymmetric) molecules with a bulky appendant or an additional ring structure; that is, the pyramidalization seems to be strongly dependent on the structure.

Scheme 2. Resonance Structures for Planar Amides

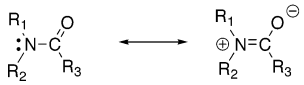

There have been few studies of pyramidalization of amides in solution. In this paper, we evaluate the planarity of the amide groups of 7-azabicyclo[2.2.1]heptane derivatives in the solution structures and compare the findings with the solid-state structures and computed gas-phase structures. An N−C(O) amide bond has a double bond character, which is conventionally interpreted in terms of resonance hybrid structures (Scheme 2). Nitrogen-pyramidalization would lead to a reduction of the amide double bond character. Hitherto, discussions favoring[16] and disfavoring[17] the significance of such resonance structures have focused only on planar amides. It will be intriguing to examine the relevance of the amide resonance model to nitrogen-pyramidal amides.

Results and Discussion

Crystal Structures of Amides of 7-Azabicyclo[2.2.1]-heptane. We synthesized various bicyclic (**1a**−**g**, **2a**−**e**, **3a**, and **4a**−**e**) and monocyclic (**5a**−**g**, **6a**−**e**, **7a**−**e,** and **8a**−**e**) amides, as depicted in Figure 3. We determined single-crystal X-ray diffraction structures of some of the amides.[18] The planarity of amide nitrogen can be represented in terms of two angle parameters: the sum of the three valence angles around the nitrogen atom (θ) and the hinge angle (α) of the N-substituent (i.e., the carbonyl carbon atom) with respect to the plane defined by the nitrogen atom and the two adjacent carbon atoms (Figure 4).[19] The angle θ of the ideal trigonal planar nitrogen atom is 360°. The hinge angle α is between 180° (pure sp^2) and 125° (pure sp^3).

Two torsion angles, ω_1 (R_3CNR_2) and ω_2 ($OCNR_1$), and the twist angle τ, which is the mean value of ω_1 and ω_2, are indicative for measuring the amount of twist about the N−C(O) bond.[20] Angle parameters in our single-crystal X-ray diffraction structures of some *N*-benzoyl-7-azabicyclo[2.2.1]heptane amides are shown in Table 1, together with the structural parameters of the four previously reported amide derivatives of 7-azabicyclo-[2.2.1]heptane (**G**−**J**).[13−15] 7-Azabicyclo[2.2.1]heptane amides (**1a**, **1c**, **1d** and **1e**) showed significant pyramidalization of the amide nitrogen atom: $\theta = 349.5$ and $\alpha = 153.2$ (i.e., the out-of-plane angle is 26.8°) for **1a** (X = H),[18,21] $\theta = 346.2$, $\alpha = 149.0$ (i.e., the out-of-plane angle is 31.0°) for **1c** (X = CH_3),[22] $\theta = 349.0$, $\alpha = 152.4$ (i.e., the out-of-plane angle is 27.6°) for

(5) Bashore, C. G.; Samardjiev, I. V.; Bordner, J.; Coe, J. W. *J. Am. Chem. Soc*. **2003**, *125*, 3268−3272.
(6) (a) Yamada, S. *Angew. Chem., Int. Ed. Engl.* **1993**, *32*, 1083−1085. (b) Yamada, S. *J. Org. Chem*. **1996**, *61*, 941−946. (c) Yamada, S.; Sugaki, T; Matsuzaki, K. *ibid.* **1996**, *61*, 5932−5938. (d) Review: Yamada, S. *J. Synth. Org. Chem. Jpn*. **1998**, *56*, 303−311.
(7) (a) Review: Rauk, A.; Allen, L. C.; Mislow, K. *Angew. Chem., Int. Ed. Engl*. **1970**, *9*, 400−414. (b) Shao, H.; Jiang, X.; Gantzel, P.; Goodman, M. *Chem. Biol.* **1994**, *1*, 231−234. (c) Korn, A.; Rudolph-Bohner, S.; Moroder, L. *Tetrahedron* **1994**, *50*, 1717−1730.
(8) (a) Glover, S. A.; Rauk, A. *J. Org. Chem.* **1999**, *64*, 2340−2345. (b) Glover, S. A. *Tetrahedron* **1998**, *54*, 7229−7272. (c) Glover, S. A.; Rauk, A. *J. Org. Chem*. **1996**, *61*, 2337−2345. (d) Gillson, A.-M. E.; Glover, S. A.; Tucker, D. J.; Turner, P. *Org. Biomol. Chem.* **2003**, *1* (19), 3430−3437.
(9) (a) Yamamoto, G.; Murakami, H.; Tsubai, N.; Mazaki, Y. *Chem. Lett.* **1997**, 605−606. (b) Yamamoto, G.; Tsubai, N.; Murakami, H.; Mazaki, Y. *Chem. Lett.* **1997**, 1295−1296. (c) Yamamoto, G.; Nakajo, F.; Tsubai, N.; Murakami, H.; Mazaki, Y. *Bull. Chem. Soc. Jpn*. **1999**, *72*, 2315−2326. (d) Yamamoto, G.; Nakajo, F.; Mazaki, Y. *Bull. Chem. Soc. Jpn.* **2001**, *74*, 1973−1974.
(10) (a) Jorgensen, W. M. *Chemtracts: Org. Chem.* **1990**, *3* (6), 431. (b) Rosen, M. K.; Standaert, R. F.; Galat, A.; Nakatsuka, M.; Schreiber, S. L. *Science* **1990**, *248* (4957), 863−866. (c) Review: Schreiber, S. L.; Albers, M. W.; Brown, E. J. *Acc. Chem. Res.* **1993**, *26*, 412−420. (d) Review: Fisher, G. *Chem. Soc. Rev.* **2000**, *29*, 119−127. (e) Hur, S.; Bruice, T. C. *J. Am. Chem. Soc*. **2002**, *124*, 7303−7313.
(11) Mannfors, B. E.; Mirkin, N. G.; Palmo, K.; Krimm, S. *J. Phys. Chem. A* **2003**, *107*, 1825−1832.
(12) (a) Ohwada, T.; Achiwa, T.; Okamoto, I.; Shudo, K. *Tetrahedron Lett.* **1998**, *39*, 865−868. (b) Review: Ohwada T. *Yakugaku Zasshi* **2001**, *121*, 65−77.
(13) Drew, M. G. B.; George, A. V.; Issacs, N. S.; Rzepa, H. S. *J. Chem. Soc., Perkin Trans. 1* **1985**, 1277−1284.
(14) Fletcher, S. R.; Baker, R.; Chambers, M. S.; Herbert, R. H.; Hobbs, S. C.; Thomas, S. R.; Verrier, H. M.; Watt, A. P.; Ball, R. G. *J. Org. Chem.* **1994**, *59*, 1771−1778.
(15) Adam, W.; Grabowski, S.; Hinz, R. F.; Lucchini, V.; Peters, E. M.; Peters, K.; Rebollo, H.; von Schneriing, H. G. *Chem. Ber*. **1987**, *120*, 2075−2079.
(16) Pauling, L. *The Nature of the Chemical Bond*, 3rd ed.; Cornell University Press: Ithaca, NY, 1960; pp 281−282.
(17) (a) Wiberg, K. B.; Laidig, K. E. *J. Am. Chem. Soc.* **1987**, *109*, 5935−5943. (b) Breneman, C. M.; Wiberg, K. B. *J. Comput. Chem.* **1990**, *11*, 361. (c) Wiberg, K. B.; Breneman, C. M. *J. Am. Chem. Soc.* **1992**, *114*, 831−840. (d) Wiberg, K. B. *Acc. Chem. Res.* **1999**, *32*, 922−929.
(18) Some of the data have been presented in ref 12a.
(19) The two angle parameters, θ and α, are not independent. On the basis of the structural data shown in Table 1, θ showed a high correlation with α (regression coefficient, $r = 0.92$).
(20) (a) Winkler, F. K.; Dunitz, J. D. *J. Mol. Biol.* **1971**, *59*, 169−182. (b) Dunitz, J. D.; Winkler, F. K. *Acta Crystallogr*. **1975**, *B31*, 251−263.

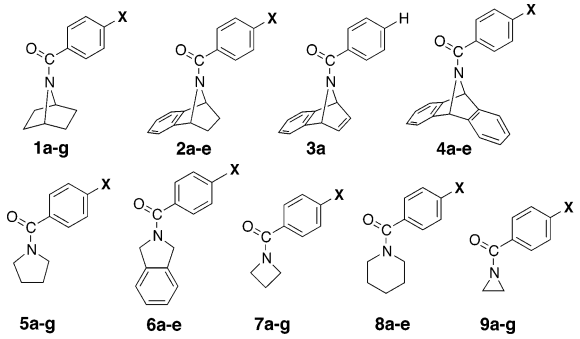

a: X = H, **b**: X = OCH_3, **c**: X = CH_3, **d**: X = Cl, **e**: X = NO_2, **f**: X = F, **g**: X = CN.

Figure 3. Bicyclic and monocyclic amides in this study.

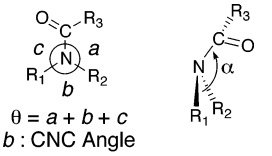

Figure 4. Definition of Angle Parameters.

Table 1. Selected Crystal Structural Data of Cyclic Amides[a]

	CNC (deg)	θ (deg)	α (deg)	N–C bond (Å)	ω_1 (deg)	ω_2 (deg)	$\|\tau\|$[b] (deg)
1a[c]	97.2(2)	349.5(2)	153.2	1.356(3)	+40.0(3)	−9.0(3)	15.5(3)
1c	97.1(1)	346.2(2)	149.0	1.361(2)	+35.9(3)	−16.3(3)	9.8(3)
1d	97.6(2)	349.0(2)	152.4	1.352(4)	−31.8(4)	+14.8(4)	8.5(4)
1e[c,d]	96.9(2)	347.1(3)	150.2	1.354(4)	+38.7(4)	−12.7(5)	13.0(5)
	97.8(2)	350.1(3)	153.8	1.350(4)	+29.1(5)	−15.4(5)	6.9(5)
4a[c]	96.6(2)	347.5(3)	150.6	1.343(4)	+35.9(5)	−14.2(6)	10.9(6)
5b	111.5(2)	359.2(2)	171.3	1.345(3)	+8.2(3)	−2.2(3)	3.0(3)
5e[c]	111.6(2)	359.3(2)	172.5	1.337(2)	−0.7(4)	−13.3(4)	7.0(4)
7c	94.6(3)	354.2(3)	161.0	1.339(4)	−22.8(6)	+13.1(5)	4.9(6)
8d	113.0(2)	358.1(2)	168.2	1.360(3)	+0.1(4)	+18.8(3)	9.5(4)
G[e]	95.2(2)	343.7(5)	146.6	1.352(8)	−44.6	+11.2	16.7
H[e]	97.6(2)	351.2(4)	155.7	1.373(7)	+24.6	−17.4	3.6
I[f]	98.0(5)	339.0	140.9	1.357	+27.7	−35.7	4.0
J[g]	94.7	328.5	132.1	1.382	+34.5	−38.3	1.9

[a] Standard deviations are shown in parentheses. [b] Reference 20. [c] Reference 12a. [d] Two kinds of molecules are involved in a unit cell. [e] Reference 13. The codes of **G** and **H** in the Cambridge Structural Database are DELYOI and DELYUO, respectively. [f] Reference 14. The code of **I** in the Cambridge Structural Database is SUMYOO. [g] Reference 15. The code of **J** in the Cambridge Structural Database is FUFLUN.

1d (X = Cl),[23] and θ = 347.1 and α = 150.2 (i.e., the out-of-plane angle is 29.8°) for **1e** (X = NO_2).[24] In contrast, *N*-aroylpyrrolidines (**5b** (X = OCH_3) and **5e** (X = NO_2)), which are the amide derivatives of a monocyclic five-membered amine, are also nonplanar in the solid state; that is, they show pyramidalization, but to a much lesser extent than the bicyclic compounds: θ = 359.2 and α = 171.3 (i.e., the out-of-plane angle is 8.7°) for **5b**,[25] θ = 359.3 and α = 172.5 (i.e., the out-of-plane angle is 7.5°) for **5e**.[18,26] The crystal structure of **5e** was previously studied,[27] and the present structural values such as the θ value of **5e** were consistent with those previously reported. Thus, the angles θ of the 7-azabicyclo[2.2.1]heptane derivatives (**1a**, **1c**, **1d**, **1e**) and the dibenzo derivative (**4a** (X = H, θ = 347.5 and α = 150.6)),[28] as well as that of azetidine amide **7c** (X = CH_3, θ = 354.2 and α =161.0),[29] apparently indicate an intermediate character of the nitrogen atom between sp^3 (ideally, θ = 328.4°) and sp^2 (ideally, θ = 360°), while the nitrogen atom of the monocyclic amides (**5b** and **5e**) is very close to sp^2 in character. The twist angles $|\tau|$ of the amide plane are also shown in Table 1: bicyclic amides **1a**, 15.5°; **1c**, 9.8°; **1d**, 8.5°; **1e**, 13.0° and 6.9°; **4a**, 10.9°; monocyclic amides **5b**, 3.0°; **5e**, 7.0°; **7c**, 4.9°. Generally, 7-azabicyclo[2.2.1]heptane amides have $|\tau|$ values larger than those of the monocyclic amides (except piperidine amide **8d**).[30] This is consistent with enhanced pyramidalization of the bicyclic compounds as compared with the monocyclic amides.

Rotational Barriers of Monocyclic and Bicyclic Amides. Rotational barriers with respect to the amide bond, the free energy of activation ($\Delta G^{\ddagger}$), can be measured to probe the planarity of amides in solution. Rotational barriers about the C−N amide bonds of *N*-benzoyl bicyclic and monocyclic amides were evaluated by variable-temperature ^{1}H NMR spectroscopy.[32] First, the rotational barriers were elucidated by a coalescence temperature method ($\Delta G^{\ddagger}_c$) (Table 2) (Figure 5).

(21) Crystallographic data for *N*-benzoyl-7-azabicyclo[2.2.1]heptane **1a**. $C_{13}H_{15}NO$, M_r = 201.27, 0.20 × 0.10 × 0.40 mm, monoclinic, space group $P2_1/n$, a = 6.217(2) Å, b = 13.380(2) Å, c = 13.258(2) Å, β = 92.48(2)°, V = 1101.8(4) Å^3, Z = 4, D_x = 1.213 g/cm^3, $2\theta_{max}$ = 135.2°, T = 296 K, μ(Cu Kα) = 6.02 cm^{-1}, F_{000} = 432.00, Rigaku AFC5S diffractometer, $\omega-2\theta$ scans, 2270 reflections measured, 2071 unique, 1453 with $I > 3.0\sigma(I)$, 137 variables, R = 0.042, R_w = 0.037, S = 2.81, $(\Delta/\sigma)_{max}$ = 0.14, $\rho\Delta_{max}$ = 0.14 eÅ^{-3}, $\Delta\rho_{min}$ = −0.11 eÅ^{-3}.

(22) Crystallographic data for *N*-(*p*-toluoyl)-7-azabicyclo[2.2.1]heptane **1c**: $C_{14}H_{17}NO$, M_r = 215.29, 0.40 × 0.30 × 0.25 mm, monoclinic, space group $P2_1/c$, a = 6.922(1) Å, b = 14.335(3) Å, c = 11.798(2) Å, β = 98.850(2)°, V = 1156.7(4) Å^3, Z = 4, D_x = 1.236 g/cm^3, $2\theta_{max}$ = 57.2°, T = 120 K, μ(Mo Kα) = 0.077 cm^{-1}, F_{000} = 464.00, Bruker Smart 1000 CCD, 6949 reflections measured, 2722 unique, 2606 with ($I > 2.0\sigma(I)$, 2θ < 57.21°), 145 variables, R = 0.048, R_w = 0.064, S = 0.85, $(\Delta/\sigma)_{max}$ = 0.001, $\rho\Delta_{max}$ = 0.21 eÅ^{-3}, $\Delta\rho_{min}$ = −0.28 eÅ^{-3}.

(23) Crystallographic data for *N*-(*p*-chlorobenzoyl)-7-azabicyclo[2.2.1]heptane **1d**: $C_{13}H_{14}ClNO$, M_r = 235.71, 0.40 × 0.40 × 0.40 mm, monoclinic, space group $P2_1/c$, a = 6.842(2) Å, b = 14.423(4) Å, c = 11.783(3) Å, β = 99.761(4)°, V = 1145.9(6) Å^3, Z = 4, D_x = 1.366 g/cm^3, $2\theta_{max}$ = 56.4°, T = 163 K, μ(Mo Kα) = 0.310 cm^{-1}, F_{000} = 496.00, Bruker Smart 1000 CCD, 6687 reflections measured, 2625 unique, 2518 with ($I > 2.0\sigma(I)$, 2θ < 56.4°), 145 variables, R = 0.046, R_w = 0.071, S = 1.04, $(\Delta/\sigma)_{max}$ = 0.001, $\rho\Delta_{max}$ = 0.26 eÅ^{-3}, $\Delta\rho_{min}$ = −0.39 eÅ^{-3}.

(24) Crystallographic data for *N*-(*p*-nitrobenzoyl)-7-azabicyclo[2.2.1]heptane **1e**: $C_{13}H_{14}N_2O_3$, M_r = 246.27, 0.15 × 0.15 × 0.40 mm, monoclinic, space group $C2/c$, a = 47.660(5) Å, b = 6.9459(9) Å, c = 14.622(1) Å, β = 90.135(8)°, V = 4840.4(9) Å^3, Z = 16, D_x = 1.352 g/cm^3, $2\theta_{max}$ = 120.1°, T = 296 K, μ(Cu Kα) = 8.07 cm^{-1}, F_{000} = 2080.00, Rigaku AFC7S diffractometer, $\omega-2\theta$ scans, 4013 reflections measured, 3958 unique, 2362 with $I > 3.0\sigma(I)$, 326 variables, R = 0.042, R_w = 0.039, S = 1.73, $(\Delta/\sigma)_{max}$ = 0.06, $\rho\Delta_{max}$ = 0.15 eÅ^{-3}, $\Delta\rho_{min}$ = −0.20 eÅ^{-3}.

(25) Crystallographic data for *N*-(*p*-anisoyl)pyrrolidine **5b**: $C_{12}H_{15}NO_2$, M_r = 205.26, 0.40 × 0.24 × 0.15 mm, monoclinic $P2_1/c$, a = 13.002(3) Å, b = 6.533(1) Å, c = 13.755(3) Å, β = 115.796(3)°, V = 1055.2(4) Å^3, Z = 4, D_x = 1.292 g/cm^3, $2\theta_{max}$ = 57.3°, T = 173 K, μ(Cu Kα) = 0.88 cm^{-1}, F_{000} = 444.00, Bruker Smart 1000 CCD, 6398 reflections measured, 2466 unique, 2254 with ($I > 2.0\sigma(I)$, 2θ < 57.3°), 136 variables, R = 0.048, R_w = 0.070, S = 0.67, $(\Delta/\sigma)_{max}$ = 0.001, $\rho\Delta_{max}$ = 0.37 eÅ^{-3}, $\Delta\rho_{min}$ = −0.46 eÅ^{-3}.

(26) Crystallographic data for *N*-(*p*-nitrobenzoyl)pyrrolidine **5e**: $C_{11}H_{12}N_2O_3$, M_r = 220.23, 0.40 × 0.25 × 0.15 mm, monoclinic, space group $P2_1/n$, a = 12.5540(8) Å, b = 6.138(1) Å, c = 14.6228(7) Å, β = 111.312(4)°, V = 1049.7(2) Å^3, Z = 4, D_x = 1.393 g/cm^3, $2\theta_{max}$ = 135.1°, T = 296 K, μ(Cu Kα) = 8.61 cm^{-1}, F_{000} = 464.00, Rigaku AFC7S diffractometer, $\omega-2\theta$ scans, 2182 reflections measured, 2085 unique, 1556 with $I > 2.0\sigma(I)$, 145 variables, R = 0.042, R_w = 0.044, S = 2.62, $(\Delta/\sigma)_{max}$ = 0.02, $\rho\Delta_{max}$ = 0.13 eÅ^{-3}, $\Delta\rho_{min}$ = −0.18 eÅ^{-3}.

(27) Pinto, B. M.; Grindley, T. B.; Szarek, W. A. *Magn. Reson. Chem.* **1986**, *24*, 323−331.

(28) Crystallographic data for *N*-benzoyldibenzo-7-azabicyclo[2.2.1]heptadiene **4a**: $C_{21}H_{15}NO$, M_r = 297.36, 0.25 × 0.25 × 0.10 mm, monoclinic, space group $P2_1/a$, a = 15.541(3) Å, b = 6.1350(7) Å, c = 16.801(2) Å, β = 91.45(1)°, V = 1601.3(4) Å^3, Z = 4, D_x = 1.233 g/cm^3, $2\theta_{max}$ = 120.1°, T = 296 K, μ(Cu Kα) = 5.94 cm^{-1}, F_{000} = 624.00, Rigaku AFC7S diffractometer, $\omega-2\theta$ scans, 2742 reflections measured, 2634 unique, 1635 with $I > 3.0\sigma(I)$, 209 variables, R = 0.048, R_w = 0.057, S = 2.51, $(\Delta/\sigma)_{max}$ = 0.04, $\rho\Delta_{max}$ = 0.15 eÅ^{-3}, $\Delta\rho_{min}$ = −0.15 eÅ^{-3}.

(29) Crystallographic data for *N*-toluoylazetidine **7c**: $C_{11}H_{13}NO$, M_r = 175.23, 0.40 × 0.30 × 0.30 mm, orthorhombic, space group $P2_12_12_1$, a = 7.661(2) Å, b = 10.758(3) Å, c = 11.453(3) Å, β = 90.0°, V = 943.9(5) Å^3, Z = 4, D_x = 1.233 g/cm^3, $2\theta_{max}$ = 57.1°, T = 163 K, μ(Cu Kα) = 0.079 cm^{-1}, F_{000} = 376.00, Bruker Smart 1000 CCD, 5680 reflections measured, 1318 unique, 2004 with ($I > 2.0\sigma(I)$, 2θ < 57.1°), 119 variables, R = 0.055, R_w = 0.075, S = 0.73, $(\Delta/\sigma)_{max}$ = 0.018, $\rho\Delta_{max}$ = 0.27 eÅ^{-3}, $\Delta\rho_{min}$ = − 0.33 eÅ^{-3}.

Table 2. Experimental Rotational Barriers Evaluated by the Coalescence Temperature Method ($\Delta G^{\ddagger}_c$) and by Line Shape Analysis ($\Delta G^{\ddagger}$)

		coalescence method			line shape analysis	
	χ	T_c[a] (°C)	$\Delta\nu$ (Hz)	$\Delta G^{\ddagger}_c$[b] (kcal/mol)	$\Delta G^{\ddagger}_{25°C}$[c,d] (kcal/ mol)	$\Delta G^{\ddagger}_{60°C}$[c,e] (kcal/mol)
		N-Aroyl-7-azabicyclo[2.2.1]heptanes				
1a	H	61.5	294.8	15.3	15.0	15.3
1b	OCH_3	42.3	236.5	14.6	14.5	14.6
1c	CH_3	52.8	267.0	15.0	15.0	15.0
1d	Cl	56.7	304.6	15.1	14.9	15.1
1e	NO_2	70.1	372.3	15.6	15.4	15.5
1f	F	52.8	288.1	14.9		
1g	CN	67.1	361.6	15.5		
		N-Aroyl-7-azabenzobicyclo[2.2.1]heptanes				
2a	H	63.1	258.8	15.5		
2b	OCH_3	44.1	202.0	14.7		
2c	CH_3	56.5	226.7	15.3		
2d	Cl	59.3	263.1	15.3		
2e	NO_2	72.8	328.1	15.8		
		N-Aroyl-7-azabenzobicyclo[2.2.1]heptadienes				
3a	H	80.4	205.4	16.5		
		N-Aroyl-7-azadibenzobicyclo[2.2.1]heptadienes				
4a	H	67.7	229.5	15.8		
4b	OCH_3	47.7	178.2	15.0		
4c	CH_3	61.3	203.3	15.6		
4d	Cl	66.0	241.7	15.7		
4e	NO_2	80.3	305.8	16.2		
		N-Aroylpyrrolidines				
5a	H	79.4	101.3	16.9	17.1	16.6
5b	OCH_3	57.3	61.0	16.2	15.7	16.1
5c	CH_3	71.7	83.0	16.7	16.7	16.6
5d	Cl	77.5	100.7	16.8	16.6	16.7
5e	NO_2	94.7	138.6	17.5	17.3	17.3
5f	F	71.9	93.7	16.6		
5g	CN	91.9	133.7	17.4		
		N-Aroylisoindoles				
6a	H	87.1	119.3	17.2		
6b	OCH_3	64.2	84.5	16.3		
6c	CH_3	78.5	103.5	16.9		
6d	Cl	84.3	118.1	17.1		
6e	NO_2	101.5	149.8	17.8		
		N-Aroylazetidines				
7a	H	53.3	57.1	16.0		
7b	OCH_3	46.7	82.7	15.4		
7c	CH_3	50.7	69.9	15.7		
7d	Cl	49.6	56.5	15.8		
7e	NO_2	47.8	34.5	16.0		
		N-Aroylpiperidines				
8a	H	53.6	179.1	15.3		
8b	OCH_3	29.6	135.2	14.3		
8c	CH_3	44.9	159.9	14.9		
8d	Cl	49.7	177.3	15.1		
8e	NO_2	68.9	219.4	15.9		

[a] The error is ±1.0 °C. [b] The error is ±0.4 kcal/mol. [c] The error is ±0.3 kcal/mol. [d] Rotational energies estimated at 25 °C. [e] Rotational energies estimated at 60 °C.

Later we compared these rotational barriers with those obtained by full line shape analysis and confirmed the reliability of the results obtained by the coalescence temperature method (vide infra). Two bridgehead protons (in the cases of the bicyclic compounds) or four protons which are bonded to the carbons adjacent to the nitrogen (in the cases of the monocyclic compounds) are nonequivalent when amide rotation is so slow that each signal can be distinguished on the NMR time scale. The rate constant k_c and $\Delta G^{\ddagger}_c$ therefore were obtained on the basis of the difference in chemical shifts ($\Delta\nu$ in Hz) of these two signals ($k_c = \pi\Delta\nu/\sqrt{2}$) and their coalescence temperature (T_c); the latter was calibrated by means of a standard method.[32c,33] Deuterated tetrachloroethane, $CDCl_2CDCl_2$, was used as a solvent throughout this work.[34] The error of the energy evaluation was ±0.4 kcal/mol. The value of the rotational barrier ($\Delta G^{\ddagger}_c$) of *N*-benzoyl-7-azabicyclo[2.2.1]heptane (**1a**, 15.3 kcal/mol) is apparently smaller than that of the corresponding monocyclic *N*-benzoylpyrrolidine (**5a**, 16.9 kcal/mol) (Figure 5). The *N*-benzoyl amides of monobenzo (**2a** and **3a**) and dibenzo (**4a**) derivatives of 7-azabicyclo[2.2.1]heptane also have rotational barriers (**2a**, 15.5; **3a**, 16.5; **4a**, 15.8 kcal/mol), smaller than that of *N*-benzoylisoindole **6a** (17.2 kcal/mol). Decreased rotational barriers of these bicyclic amides strongly suggest that the double bond character of the N−CO bond is reduced in the *N*-benzoyl derivatives of the 7-azabicyclo[2.2.1]heptane motif.[35] This observation indicates distortion of the amide planarity. Thus, we postulate that the 7-azabicyclo[2.2.1]heptane amides are pyramidalized in solution. It is noteworthy that the rotational

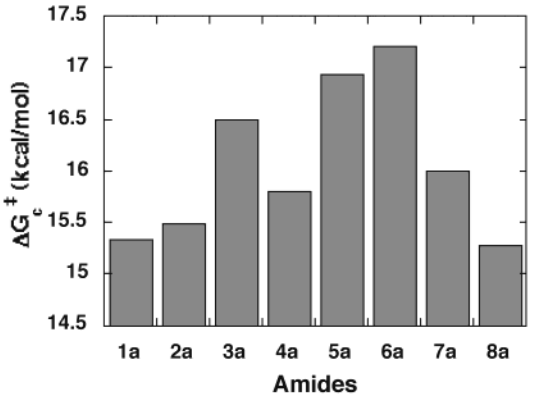

Figure 5. Rotational barriers of amides in solution, estimated by the coalescence temperature method.

(30) The parameters of the single-crystal X-ray diffraction structure of the monocyclic piperidine amide **8d** (X = Cl) were also determined: θ = 358.1°, α = 168.2°, and $|\tau|$ = 9.5° (see ref 31). The magnitudes of deviation of θ and α are similar to those of pyrrolidine amides. As indicated by the magnitudes of the α and $|\tau|$ values, the piperidine amide (**8d**) is a pyramidal amide with enhanced twisting (see ref 35). The B3LYP/6-31G* optimized structure of *N*-benzoylpiperidine **8a** also exhibited slight nitrogen-pyramidalization and apparent twisting of the amide bond: θ = 356.3°, α = 162.0°, and $|\tau|$ = 15.7°.

(31) Crystallographic data for *N*-(*p*-chlorobenzoyl)piperidine **8d**: $C_{12}H_{14}ClNO$, M_r = 223.70, 0.40 × 0.40 × 0.30 mm, monoclinic, space group $P2_1/c$, a = 10.093(2) Å, b = 10.011(2) Å, c = 11.451(3) Å, β = 108.627(3)°, V = 1096.4(5) Å^3, Z = 4, D_x = 1.355 g/cm^3, $2\theta_{max}$ = 56.8°, T = 273 K, μ(Mo Kα) = 0.319 cm^{-1}, F_{000} = 472.00, Bruker Smart 1000 CCD, 6545 reflections measured, 2555 unique, 2405 with ($I > 2.0\sigma(I)$, $2\theta < 56.8°$), 136 variables, R = 0.050, R_w = 0.063, S = 0.65, $(\Delta/\sigma)_{max}$ = 0.004, $\rho\Delta_{max}$ = 0.43 eÅ^{-3}, $\Delta\rho_{min}$ = −0.58 eÅ^{-3}.

(32) (a) Mannschreck, A.; Münsch, H.; Mattheus, A. *Angew. Chem., Int. Ed. Engl.* **1966**, *5*, 728. (b) Mannschreck, A.; Münsch, H. *Angew. Chem., Int. Ed. Engl.* **1967**, *6*, 984−985. (c) Review: Stewart, W. E.; Siddall, T. H., III. *Chem. Rev.* **1970**, *70*, 517−551. (d) Oki, M. *Applications of Dynamic NMR Spectroscopy to Organic Chemistry*; VCH Publishers: Deerfield, 1985; Vol. 4.

(33) Ammann, C.; Meier, P.; Merbach, A. E. *J. Magn. Reson.* **1982**, *46*, 319−321.

(34) The effect of solvent polarity seems to be small, as judged from the small effect on the rotational barriers of the *N*-nitrosoamines of the similar bicyclic systems (see: Ohwada, T.; Miura, M.; Tanaka, H.; Sakamoto, S.; Yamaguchi, K.; Ikeda, H.; Inagaki, S. *J. Am. Chem. Soc.* **2001**, *123*, 10164−10172).

(35) The significantly low rotational barrier of the six-membered piperidine *N*-benzoylamide (**8a**, 15.3 kcal/mol, the coalescence temperature method) is consistent with values previously obtained (see ref 36a). As proposed previously (see ref 36b−d), this small rotational barrier is likely to be due to 1,3-allylic strain between equatorial protons of the piperidine ring and *ortho*-protons of the phenyl ring or the oxygen atom of the amide in the ground state; this strain destabilizes the ground-state structure, leading to a reduction of the energy gap with the rotational TS. This allylic strain leads to twisting of the amide bond, resulting in nitrogen-pyramidalization (see ref 30).

barrier of the azetidine derivative (**7a**) (16.0 kcal/mol) is as small as those of the bicyclic amides (**1a**, **2a**, **3a**, **4a**), while the *N*-aroylazetidine (**7c**) has an nitrogen-pyramidal amide structure in the solid state (see Table 1).

The barriers to rotation about the C−N bond in bicyclic (**1a**) and monocyclic (**5a**) benzamides were also determined by full line shape analysis[37] on the basis of the experimental NMR spectra of the bridgehead protons (Table 2). Line shape analysis was performed by visual matching of the simulated spectra with the experimental spectra. Rate constants were obtained at several temperatures, and $\Delta H^{\ddagger}$ and $\Delta S^{\ddagger}$ were calculated by least-squares analysis of the Eyring plots, from which the $\Delta G^{\ddagger}$ values at a specific temperature (e.g., 60 °C) were obtained. The error limit for $\Delta G^{\ddagger}$ was ±0.3 (or 0.2) kcal/mol.[37] The magnitudes of the rotational barriers of **1a** ($\Delta G^{\ddagger}_{60°C}$, 15.3 kcal/mol) and **5a** ($\Delta G^{\ddagger}_{60°C}$, 16.6 kcal/mol) obtained by the line shape analysis are in good agreement with those obtained by the coalescence temperature method.

Generality of Solution Structures

Electronic Effect. To generalize the trend seen above in the unsubstituted amides, we examined *para*-substituted benzamides. We evaluated the rotational barriers of *N*-aroyl-7-azabicyclo[2.2.1]heptanes bearing representative electron-donating (**1b**: OCH_3, **1c**: CH_3) or electron-withdrawing (**1d**: Cl, **1e**: NO_2, **1f**: F, **1g**: CN) substituents on the benzoyl group using the coalescence temperature method, and also by full line shape analysis of their NMR spectra (Table 2). As in the case of the unsubstituted compound (**1a**), the rotational barriers obtained by the two methods coincided well for the substituted compounds (Table 2). We compared the rotational barriers of **1b**−**g** with those of the corresponding pyrrolidine amides (**5b**−**g**). It is clear that, for all substituents, the bicyclic amides (**1b**−**g**) have lower rotational barriers than the corresponding monocyclic pyrrolidine amides (**5b**−**g**) do (see Figure 6A). The magnitudes of the barriers of **5b** and **5e** are consistent with those previously reported.[27,38a] Thus, it is likely that the bicyclic amides (**1a**−**g**) show similar structural features, that is, nitrogen-pyramidalization, in solution irrespective of the substituent. A similar tendency is observed in Figure 6B; that is, benzene-fused bicyclic amides (**2a**−**e** and **4a**−**e**) have smaller rotational barriers than the corresponding monocyclic amides, *N*-aroylisoindoles (**6a**−**e**), do.

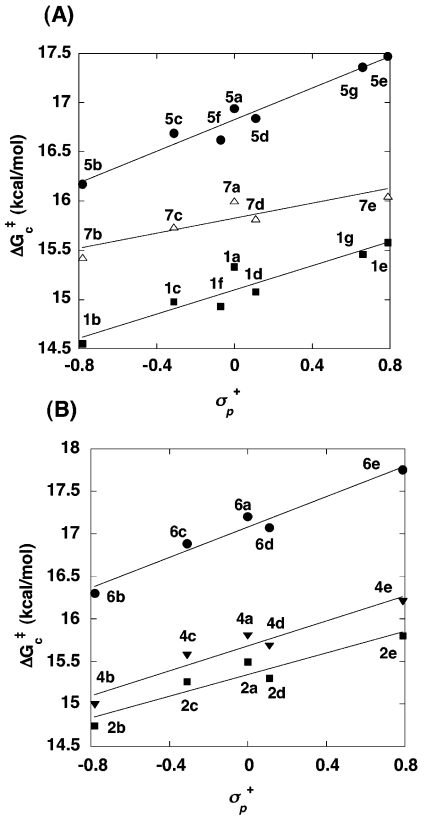

Figure 6. Relationship between rotational barriers $\Delta G_c^{\ddagger}$ (kcal/mol) of substituted benzamides and Hammett's σ_p^+ values of the corresponding substituents. (A) Aliphatic ring system: **1a**−**g**, **5a**−**g**, and **7a**−**e**. (B) Benzene-fused ring system: **2a**−**e**, **4a**−**e**, and **6a**−**e**.

The rotational barriers of azetidine amides (**7b**−**e**) were also determined by the coalescence temperature method (Figure 6A). The magnitudes of the rotational barriers of **7a**−**e** are larger than those of the bicyclic amides (**1a**−**g**) in all cases, for corresponding substituents. The rotational barriers of the *N*-aroyl amides with a different ring system **1a**−**g**, **2a**−**e**, **4a**−**e**, **5a**−**g**, **6a**−**e**, and **7a**−**e** showed good correlations with the Hammett's σ_p^+ constants although the correlation in the case of **7a**−**e** is relatively poor.[38,39] The slopes of the regression lines (ρ^+) are of similar magnitude, indicating the involvement of similar electronic effects in the rotation process.

Comparison of Observations with Calculated Geometries and Calculated Rotational Barriers of Bicyclic and Monocyclic Amides. Structures of bicyclic and monocyclic amides were optimized by means of density functional theory (DFT) calculations (B3LYP/6-31G*) (Figures 7 and 8; see also the Supporting Information).[40] The minimum energy structure of

(36) (a) Buhleier, E.; Wehner, W.; Vögtle, F. *Chem. Ber.* **1979**, *112*, 559−566. (b)Hoffmann, R. W. *Angew. Chem., Int. Ed. Engl.* **1992**, *31*, 1124−1134. (c) Johnson, R., A. *J. Org. Chem.* **1968**, *33*, 3627−3632. (d) Review: Johnson, F. *Chem. Rev.* **1968**, *68*, 375−413.

(37) Line shape analysis was carried out with a program, gNMR version 4.1, Adept Scientific plc., UK for PC. Experimentally obtained spectra were converted in gNMR, the selected region was smoothed, and the baseline was corrected as appropriate. The input for the exchange calculations included the relative chemical shifts of the bridgehead protons for **1a**−**e** (numbered 1-1, 1-2, respectively) or α protons for **5a**−**e** (numbered 1-1, 1-2, respectively), line widths at half-height and coupling constants. Temperature dependences of isomer populations, differences in chemical shifts, and T_2 values were properly taken into account. The exchange description (1-1 → 1-2, 1-2 → 1-1) and the arbitrary values of the rate constant (k) were also required. Chemical-exchange calculations were performed with the rate constant fixed. The rate constants were obtained by visual matching of the experimental spectra with those calculated for various k. Activation parameters and errors for the process of line shape matching were calculated from the Eyring equation: $\ln(k/T) = -(\Delta H^{\ddagger}/RT) + (\Delta S^{\ddagger}/R) + \ln(k_B/h)$; that is, $\ln(k/T) = (-\Delta H^{\ddagger}/1000R) \times (1000/T) + (\Delta S^{\ddagger}/R) + \ln(k_B/h)$, where T is the simulation temperature, R is the gas constant (1.98719 cal K^{-1} mol^{-1}), k_B is the Boltzmann constant (3.29986 × 10^{-24} cal K^{-1}), and h is Planck's constant (1.58369 × 10^{-34} cal s). Parameters were obtained from the unbiased estimates of the standard deviations of least-squares parameters and are reported at the 95% confidence level. $\Delta G^{\ddagger}$ was obtained from the following equation: $\Delta G^{\ddagger} = \Delta H^{\ddagger} - T\Delta S^{\ddagger}$, and errors in $\Delta G^{\ddagger}$ values were evaluated as the sum of the errors in $\Delta H^{\ddagger}$ and the product of those in $\Delta S^{\ddagger}$ and T. The average of errors in $\Delta G^{\ddagger}$ values was calucalated to be 0.3 (typically 0.2) kcal/mol in the Eyring equation plot. The obtained value of the $\Delta G^{\ddagger}$ for **5e** in this method is consistent with that previously obtained by a different line shape analysis (see ref 27).

(38) (a) Jackman, L., M.; Kavanagh, T. E.; Haddon, R. C. *Org. Magn. Reson.* **1969**, *1*, 109−123. (b) Fong, C. W.; Lincoln, S. F.; Williams, E. H. *Aust. J. Chem.* **1978**, *31*, 2615−2621. (c) Drakenberg, T. *Tetrahedron Lett.* **1972**, *18*, 1743−1746. (d) Gryff-Keller, A.; Terpinski, J.; Zajaczkowska-Terpinska, E. *Pol. J. Chem.* **1980**, *54*, 1465−1471. (e) Turnbull, M. M.; Nelson, D. J.; Lekouses, W.; Sarnov, M. L.; Tartarini, K. A.; Huang, T. *Tetrahedron* **1990**, *46*, 6613−6622.

(39) Regression coefficients (r) between the experimental rotational barriers and Hammett's σ_p^+ constants (Figure 6) are as follows: **1a**−**g**, 0.94; **2a**−**e**, 0.95; **4a**−**e**, 0.97; **5a**−**g**, 0.98; **6a**−**e**, 0.98; **7a**−**e**, 0.89.

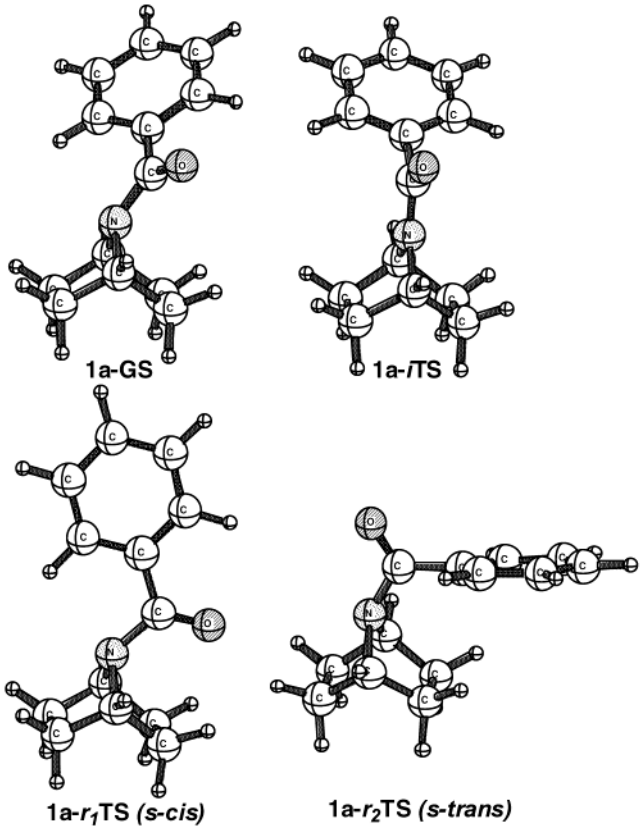

Figure 7. Calculated ground and transition state structures of *N*-benzoyl bicylic amide **1a** at the B3LYP/6-31G* level.

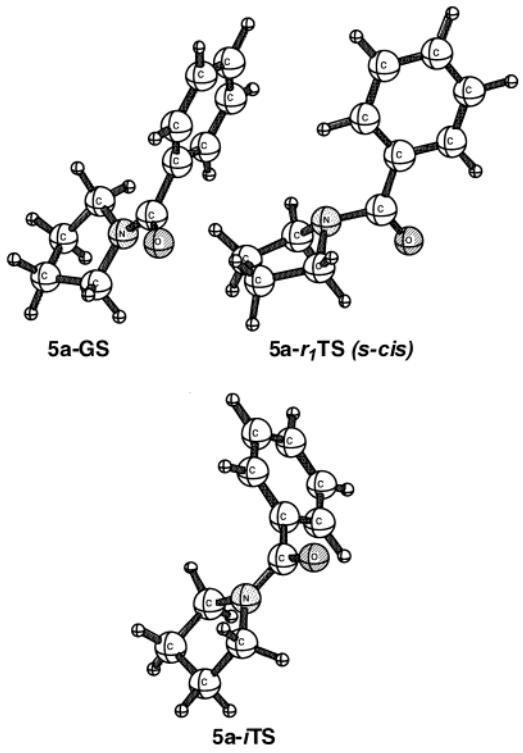

Figure 8. Calculated ground and transition state structures of *N*-benzoyl monocyclic amide **5a** at the B3LYP/6-31G* level.

the bicyclic amide **1a** (**1a-GS**) was found to be nitrogen-pyramidal (calculated θ and α are 343.5° and 146.0°, respectively)(Figure 7). On the other hand, the ground minimum structures of the monocyclic *N*-benzoylpyrrolidine amides are also pyramidalized, but to a lesser extent (for **5a-GS**, calculated θ and α are 356.1° and 161.7°, respectively)(Figure 8). Although there is a tendency that the degree of nitrogen-pyramidalization of the calculated structures is consistently larger than that of the solid-state structures, the relative order of the magnitudes of pyramidalization of the calculated structures is consistent with that found in the solid-state structures: 7-azabicyclo[2.2.1]-heptane amides (**1a**−**g**) > azetidine amides (**7a**−**g**) > pyrrolidine amides (**5a**−**g**).

Furthermore, we optimized two possible transition structures of rotation about the N−C(O) bond in the amide group of the parent bicyclic (**1a**) and monocyclic (**5a**) amides: *s-cis* (**r_1TS**) and *s-trans* (**r_2TS**) conformations (in which the CO bond is *syn*-periplanar or *anti*-periplanar with respect to the nitrogen substituents, respectively) (Figures 7 and 8). In the case of **1a**, the *s-cis* conformer (**1a-r_1TS**) is lower in energy (B3LYP/6-311G* basis set on the basis of B3LYP/6-31G* optimized structure) than the *s-trans* conformer (**1a-r_2TS**) by 14.0 kcal/mol, so we focused on the rotation to the *s-cis* conformations of the rotated transitional amides. In the case of nonplanar monocyclic **5a**, only the *s-cis* conformer (**5a-r_1TS**) was obtained as a transition structure.

The corresponding nitrogen planar structures (**1a-*i*TS** and **5a-*i*TS**) were transitional, and the calculated inversion barriers were found to be small (2.5 kcal/mol for the bicyclic amide **1a** and 0.7 kcal/mol for the monocyclic amide **5a** (B3LYP/6-311G*)) (see Table 3). Therefore, inversion is not a rate-determining process in the amide isomerization of amide bonds, but rotation is. Calculated rotational barriers with respect to the N−CO bonds of the amides **1a**−**e** and **5a**−**e** are shown in Table 3. Table 3 also includes the values for aziridine amides (**9a**−**g**), though the small rotational barriers of these compounds could not be accessed experimentally by means of dynamic NMR methods.[41] The relative orders of magnitude of the calculated rotational barriers of **1a**−**g** and **5a**−**g** are consistent with those of the experimental $\Delta G^{\ddagger}_{c}$ values obtained in solution, though the calculated values are consistently smaller (by approximately 5 kcal/mol) than the experimental values. It was previously pointed out that rotational barriers of amides calculated by means of ab initio methods are consistently smaller than those measured experimentally.[42] The calculated rotational barriers of the bicyclic amides (**1a**−**g**) are smaller than those of pyrrolidine amides (**5a**−**g**) and azetidine amides (**7a**−**g**). This is consistent with the trend of the experimentally determined rotational barriers.

What are the Factors Influencing the Nitrogen-Pyramidalization of Amides? Effect of Bond Angles. Intuitively, the

(40) Frisch, M. J.; Trucks, G. W.; Schlegel, H. B.; Gill, P. M. W.; Johnson, B. G.; Robb, M. A.; Cheeseman, J. R.; Keith, T.; Petersson, G. A.; Montgomery, J. A.; Raghavachari, K.; Al-Laham, M. A.; Zakrzewski, V. G.; Ortiz, J. V.; Foresman, J. B.; Cioslowski, J.; Steranov, B. B.; Nanayakkara, A.; Challacombe, M.; Peng, C. Y.; Ayala, P. Y.; Chen, W.; Wong, M. W.; Andres, J. L.; Replogle, E. S.; Gomperts, R.; Martin, R. L.; Fox, D. J.; Binkley, J. S.; Defrees, D. J.; Baker, J.; Stewart, J. P.; Head-Gordon, M.; Gonzalez, C.; Pople, J. A. *Gaussian 94*, revision D.3; Gaussian, Inc.: Pittsburgh, PA, 1995.

(41) In the case of aziridine amides, the inversion barrier exceeds the amide rotational barrier in magnitude. (a) Anet, F. A. L.; Osyany, J. M. *J. Am. Chem. Soc.* **1967**, *89*, 352−356. (b) Boggs, G. R.; Gerig, J. T. *J. Org. Chem.* **1969**, *34*, 1484−1487.

(42) (a) Drakenberg, T.; Dahlqvist, K. J.; Forsen, S. *J. Phys. Chem.* **1972**, *76*, 2178. (b) Wiberg, K. B.; Rablen, P. R.; Rush, D. J.; Keith, T. A. *J. Am. Chem. Soc.* **1995**, *117*, 4261−4270.

Table 3. Calculated Rotation and Inversion Barriers of the Amides (kcal/mol)[a,b]

	A:6-31G* B:6-311G**		
transformation process	HF/A	B3LYP/A	B3LYP/B
N-Aroyl-7-azabicyclo[2.2.1]heptanes			
1a-GS → **1a**-r_1**TS**	9.71	10.92	10.94
1a-GS → **1a**-r_2**TS**	24.85	25.12	24.98
1a-GS → **1a**-*i***TS**	3.46	3.12	2.51
1b-GS → **1b**-r_1**TS**	8.98	10.05	10.09
1c-GS → **1c**-r_1**TS**	9.51	10.70	10.68
1d-GS → **1d**-r_1**TS**	9.52	10.77	10.84
1e-GS → **1e**-r_1**TS**	10.00	11.48	11.51
1f-GS → **1f**-r_1**TS**	9.27	10.53	10.53
1g-GS → **1g**-r_1**TS**	9.82	11.26	11.34
N-Aroylpyrrolidines			
5a-GS → **5a**-r_1**TS**	9.92	11.99	11.82
5a-GS → **5a**-*i***TS**	0.49	0.96	0.74
5b-GS → **5b**-r_1**TS**	10.14	11.98	11.47
5c-GS → **5c**-r_1**TS**	10.82	12.79	12.22
5d-GS → **5d**-r_1**TS**	10.95	12.92	12.49
5e-GS → **5e**-r_1**TS**	11.72	13.91	13.46
5f-GS → **5f**-r_1**TS**	10.59	12.67	12.18
5g-GS → **5g**-r_1**TS**	11.44	13.62	13.16
N-Aroylazetidines			
7a-GS → **7a**-r_1**TS**	10.58	11.98	11.96
7b-GS → **7b**-r_1**TS**	9.83	11.08	11.07
7c-GS → **7c**-r_1**TS**	10.39	11.76	11.61
7d-GS → **7d**-r_1**TS**	10.38	11.90	11.77
7e-GS → **7e**-r_1**TS**	10.93	12.65	12.60
7f-GS → **7f**-r_1**TS**	10.15	11.62	11.57
7g-GS → **7g**-r_1**TS**	10.74	12.41	12.39
N-Aroylpiperidines			
8a-GS → **8a**-r_1**TS**	7.86	10.54	10.69
N-Aroylaziridines			
9a-GS → **9a**-r_1**TS**	1.93	2.85	3.00
9b-GS → **9b**-r_1**TS**	1.71	2.52	2.68
9c-GS → **9c**-r_1**TS**	1.85	2.76	2.91
9d-GS → **9d**-r_1**TS**	1.80	2.77	2.95
9e-GS → **9e**-r_1**TS**	1.94	3.09	3.27
9f-GS → **9f**-r_1**TS**	1.69	2.64	2.82
9g-GS → **9g**-r_1**TS**	1.87	2.97	3.16

[a] All the structures were optimized at the B3LYP/6-31G* level. [b] Energies were corrected with scaled zero-point energy (scaled by 0.89), based on the HF/6-31G* frequency calculations.

angle strain around the nitrogen atom of 7-azabicyclo[2.2.1]-heptane would seem to be a plausible origin of the nitrogen-pyramidalization. Thus, we examined the relation between the CNC angle and the magnitude of the rotational barrier, the latter being an index of nitrogen-pyramidalization. With the crystal (Table 1) or calculated (see the Supporting Information) structural data, no correlation between the CNC angle and rotational barrier was found (Figure 9); the CNC angles of the amides of 7-azabicyclo[2.2.1]heptane (**1a**−**e**) are smaller than those of monocyclic pyrrolidine amides (**5a**−**e**), because of pinching of the ring with the ethano bridge. The CNC angles of azetidine amides (**7a**−**e**) are smaller than those of the bicyclic amides (**1a**−**e**). However, within a series of compounds bearing a particular skeleton (for example, **1a**−**e**), there is little fluctuation in the CNC angles, despite the apparent change in the rotational barriers. Thus, the CNC angle alone cannot explain the differences of rotational barrier and, consequently, nitrogen-pyramidalization.

Twisting of Amide Bonds due to Allylic Strain. A reduced CNC angle may be one of the factors influencing nitrogen-pyramidalization, but allylic strain, that is, steric repulsion of substituents on the nitrogen of the amide (the oxygen atom and

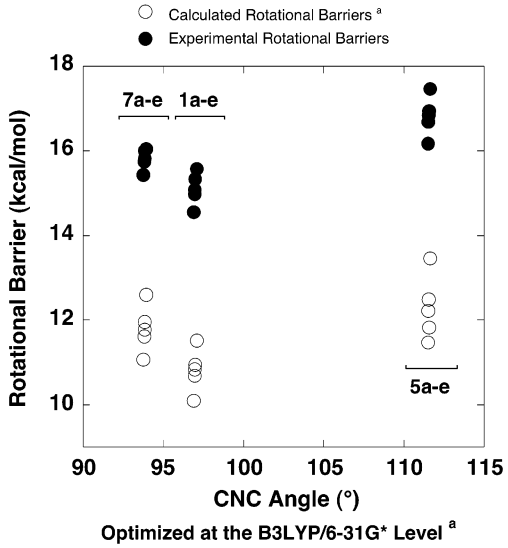

Figure 9. Relationship between calculated CNC angles and experimental or calculated rotational barriers. Calculations were performed at the B3LYP/6-311G**//B3LYP/6-31G* level.

the phenyl group in the case of the *N*-benzoylamides) from the bridgehead hydrogens of the 7-azabicyclo[2.2.1]heptane, may also contribute. This allylic strain can induce twisting about the amide N−C(O) bond.[36c,d] To assess the effect of the bulkiness of the substituents in the amide functional group, we obtained the optimized minimum structures of the amides which bear acetyl and formyl groups as N-substituents (see the Supporting Information). The minimum structures of *N*-acetyl- and *N*-formyl-7-azabicyclo[2.2.1]heptanes are nitrogen-pyramidal.[43] Furthermore, within the same bicyclic system (**1**), the calculated rotational barriers increase as the amide substituent changes from benzoyl (PhCO, **1a**) to acetyl (CH_3CO, **1h**) to formyl (HCO, **1i**) (Figure 10 and see also the Supporting Information). This is reasonable, because the electron deficiency of the carbonyl carbon centers increases in this order, leading to enhanced amide resonance (see Scheme 2), and also because the steric repulsion described above is reduced as the size of the substituent attached to the carbonyl carbon atom is decreased.[44]

The plot shown in Figure 10 suggests a general trend that the larger the degree of nitrogen-pyramidization (i.e., the smaller the angle α is), the larger the twisting of the amide is (i.e., the larger the τ is).[35] Thus, nitrogen-pyramidalization and twisting of the amide bond are strongly coupled.[45] 7-Azabicyclo[2.2.1]-heptane amides have characteristically large τ values in the calculated structures (18.3° (crystal data, 15.5°) for the benzamide **1a**, 6.2° for the acetamide **1h**, and 4.0° for the

(43) We also studied single-crystal X-ray diffraction structures (Supporting Information) of two *N*-acetyl-7-azabicyclo[2.2.1]heptane derivatives, *N*-acetyl-*endo*-2,3-di(methoxycarbonyl)-7-azabicyclo[2.2.1]heptane (**K**), and *N*-acetyldibenzo-7-azabicyclo[2.2.1]heptadiene (**L**). The structural parameters are as follows: $\theta = 344.2(3)°$, $\alpha = 146.7°$, and $|\tau| = 4.2(5)°$ for **K**; $\theta = 357.8(3)°$, $\alpha = 168.0°$, and $|\tau| = 0.2(8)°$ for **L** (see Supporting Information). We thus confirmed that these compounds exhibit nitrogen-pyramidalization in the solid state.

(44) The calculated (B3LYP/6-31G*) twist angles $|\tau|$ were as follows: **1a**, 18.3°; **1h**, 6.2°; **1i**, 4.0°; **5a**, 8.6°; **5h**, 0.5°; **5i**, 0.2°; **7a**, 11.0°; **7h**, 2.5°; **7i**, 1.5°. This reduction of the $|\tau|$ values depending on the N-substituent can be interpreted in terms of relief of the allylic strain with decrease in the size of the substituent.

(45) The combination of the effects of twisting of the amide bond and nitrogen pyramidalization would modulate the reactivities of the amide. For example, the acceleration of hydrolysis of amides was recently computationally studied: Lopez, X.; Mujika, J. I.; Blackburn, G. M.; Karplus, M. *J. Phys. Chem. A* **2003**, *107*, 2304−2315.

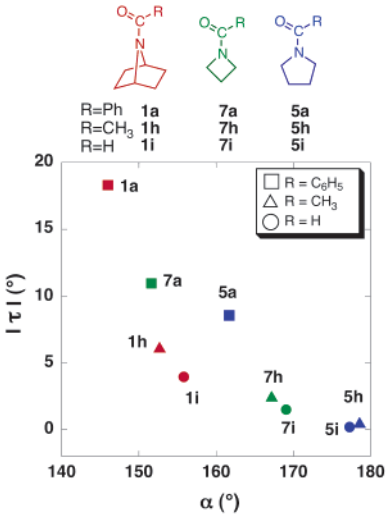

Figure 10. Correlation between nitrogen-pyramidalization (α) and amide twisting (τ), calculated at the B3LYP/6-31G* level.

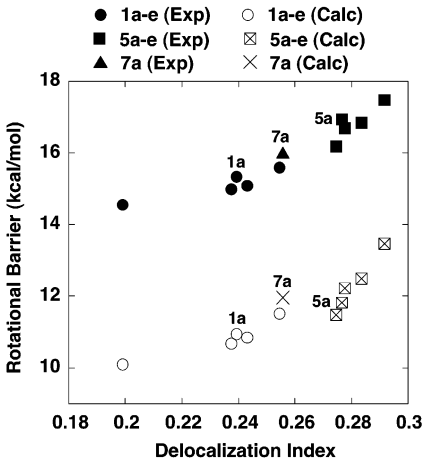

Figure 11. Relationship between electron delocalization from nN to πCO* calculated by the bond model and the experimental/calculated rotational barriers.

formamide **1i**) as compared with those of the monocyclic amides (**5a**, **5h**, and **5i**; **7a**, **7h**, and **7i**) with the same N-substituent. Thus, the low rotational barrier of *N*-benzoyl-7-azabicyclo[2.2.1]-heptane can be attributed to the twisting of the N−C(O) bond in addition to nitrogen-pyramidalization. In other words, the nitrogen nonplanarity, a reflection of the rotational barrier, is determined by the overall structural character of the molecule and not by a single structural parameter.

Electron Delocalization Estimated from a Bond Model. We tried to assess quantitatively the effect of the structural character on the favorability of the nonplanarity of amides, that is, the effect on the amide rotational barrier. In terms of electronic effects, an amide bond can be understood by applying a resonance model, that is, electron donation from the nitrogen atom to the carbonyl oxygen atom (see Scheme 2).

The electronic wave function at the HF/6-31G*//B3LYP/6-31G* level was analyzed according to the bond model method.[46,47] The delocalization index is defined as the relative ratio of the coefficient of the transferred configuration to that of the ground configuration (C_T/C_G) to show the delocalizability between the bonds. The delocalization index (C_T/C_G) for the nitrogen nonbonding orbital n_N to the vacant carbonyl π^* orbital (π^*_{CO}) was found to correlate well with the calculated and experimental rotational barriers of the *N*-benzamides (**1a**−**e**, **5a**−**e**, and **7a**) (Figure 11). The bicyclic amides **1a**−**e** have smaller delocalization indexes than the pyrrolidine amides **5a**−**e**. This corresponds well to the smaller rotational barriers of the former than the latter. Also, in the case of the azetidine amide **7a**, whose CNC angle is smaller than that of the bicyclic **1a**, **7a** does have a *larger delocalization index* and a larger rotational barrier than **1a**. Thus, this delocalization index well represents the magnitude of the *nonplanarity* of amides, which is mainly derived from a combination of *nitrogen-pyramidalization* and *amide bond twisting* (Scheme 1). Furthermore, the magnitude of the resonance stabilization, that is, the delocalization stabilization of the lone pair electrons of the nitrogen atom to the C=O π^* orbital, can determine the rotational barrier of the N−CO bond even in nitrogen-pyramidal amides.

Conclusions

We evaluated the planarity of the amide group of 7-azabicyclo-[2.2.1]heptane amides in the solid, solution, and calculated gas-phase structures. Reduction of experimental and calculated rotational barriers, as compared with those of the monocyclic pyrrolidine amides, suggested that 7-azabicyclo[2.2.1]heptane amides are intrinsically nitrogen-pyramidal. We also found a good correlation between the rotational barriers of *N*-aroyl-7-azabicyclo[2.2.1]heptanes and the Hammett's σ_p^+ constants, suggesting that similar electronic effects operate in the pyramidal amides. The magnitude of the rotational barrier in solution is a reflection of the nonplanarity. Bond model calculations showed a good correlation between the delocalization index and the rotational barrier. Thus, the pyramidalization of the amides of 7-azabicyclo[2.2.1]heptanes is a reasonable outcome of the reduction of the electron delocalization of the n_N orbital to the π^*_{CO} orbital of the amides. Nonplanarity involves nitrogen-pyramidalization derived from the CNC angle strain and twisting of the amide bond due to allylic strain. The present study results provide a fundamental basis for designing nitrogen-pyramidal peptides and understanding their properties.[12,48]

Acknowledgment. This work was supported in part by a Grant-in-Aid from the Ministry of Education, Science, Sports, Culture and Technology, Japan, and grants from the Naito Foundation, Terumo Life Science Foundation, Shimadzu Science Foundation, and The Mochida Memorial Foundation for Medical and Pharmaceutical Research. Most calculations were

(46) Bond Model for Molecules and Transition States Program. Inagaki, S.; Ikeda, H. *J. Org. Chem.* **1998**, *63*, 7820−7824. See also: (a) Inagaki, S.; Kawata, H.; Hirabayashi, Y. *Bull. Chem. Soc. Jpn.* **1982**, *55*, 3724−3732. (b) Inagaki, S.; Goto, N.; Yoshikawa, K. *J. Am. Chem. Soc.* **1991**, *113*, 7144−7146. (c) Inagaki, S.; Yoshikawa, K.; Hayano, Y. *J. Am. Chem. Soc.* **1993**, *115*, 3706−3709. (d) Inagaki, S.; Ishitani, Y.; Kakefu, T. *J. Am. Chem. Soc.* **1994**, *116*, 5954−5958.

(47) The single Slater determinant of the Hartree−Fock wave function for the electronic structure of a molecule is expanded into electron configurations. In the ground configuration, a pair of electrons occupies each bonding orbital of the bonds. Electron delocalization is expressed by mixing an electron-transferred configuration, where an electron shifts from the bonding orbital of a bond to the antibonding orbital of another. A set of bond (bonding and antibonding) orbitals gives the coefficients of the electron configurations, i.e., C_G and C_T values, and is optimized to give the maximum value of the coefficient of the ground configuration.

(48) (a) Avenoza, A.; Cativiela, C.; Busto, J. H.; Fernandez-Recio, M. A.; Peregrina, J. M.; Rodriguez, F. *Tetrahedron* **2001**, *57*, 545−548. (b) Avenoza, A.; Busto, J. H.; Peregrina, J. M.; Rodriguez, F. *J. Org. Chem.* **2002**, *67*, 4241−4249.

carried out at the Computer Center, the Institute for Molecular Science and the Computer Center of the University of Tokyo. The authors thank these computational facilities for the generous allotment of computer time.

Supporting Information Available: Full experimental details (synthesis, X-ray diffraction data and NMR data) (Figure S1 and Table S1) and calculated geometries (coordinates) and computational details (Figures S2 and S3 and Tables S2−S5). This material is available free of charge via the Internet at http://pubs.acs.org.

JA036644Z